N87-16327

A MIRROR TRANSPORT MECHANISM FOR USE AT CRYOGENIC TEMPERATURES

Kenneth W. Stark* and Meredith Wilson*

This report describes the Mirror Transport Mechanism (MTM), which supports a pair of dihedral mirrors and moves them in a very smooth and uniform scanning motion normal to a beamsplitter. Each scan is followed by a quick flyback and repeat.

Included in the report will be material selection, design, and testing of all major components of the MTM in order to meet the stringent performance requirements under cryogenic conditions and survive the launch environment of the shuttle. Areas to be discussed in detail will be those in which failures or performance anomalies occurred and their solutions. Typically, this will include (but not to be limited to) flex pivot failures during vibration testing, excessive dihedral platform sag under one "g" operation, electronic and fiber optic characteristics, and tolerancing considerations.

As of this writing, development of the mechanism has reached the final phase of thermal and vibration qualification. Environmental testing of the complete FIRAS experiment is just beginning.

INTRODUCTION

The Mirror Transport Mechanism (MTM) is an integral part of the Far Infrared Absolute Spectrophotometer (FIRAS) instrument. The FIRAS measures the spectrum of the 3 K cosmic background radiation, the interstellar dust emission, and any unknown sources in the wavelengths ranging from 100 μm to 1 cm. The FIRAS is a cryogenically cooled (LHe) rapid scan interferometer spectrophotometer. A pair of dihedral mirrors is moved with respect to a beamsplitter, producing the optical path differences which generate an interferogram. Incoming radiation, which is channeled into the interferometer by a skyhorn, is balanced against an internal reference source.

An external calibrator is also provided which when commanded will swing into place in front of the skyhorn at which time the temperature of the internal reference source is adjusted to nearly null the signal. Proper operation requires that the entire instrument be maintained at a temperature below 2 K. Thus, it is enclosed in a large dewar filled with superfluid helium at 1.8 K. Spacecraft orbit is such that complete coverage of the universe requires about 6 months. For double coverage, a lifetime of at least a year in orbit is desired. Since any power dissipated in the dewar increases boil-off of the cryogen, strict limits are placed on the allowable

*NASA Goddard Space Flight Center, Greenbelt, Maryland.

dissipation. The FIRAS power budget is 5 mW. Lifetime in orbit is reduced by about 3 days/mW.

The dihedral mirrors are mounted on the MTM platform and the MTM is designed as a basic 4 bar linkage connected by a set of 8 flexural pivots. These flex pivots are essentially frictionless and provide only a small linear restoring force. Angular rotation is low enough that expected lifetime at normal temperature is infinite. However, the entire mechanism must operate at 1.8 K for more than a year and there is no such previous experience. Flex pivots were fabricated with a special material and life-tested for more than 20 million cycles at LHe temperature and with greater than normal rotation. The MTM is driven by a unique linear motor whose only moving part is completely passive (no contact, no flexing wires). Scan operation is controlled by an optical encoder, which consists essentially of a pair of gratings having 50 lines/mm. Thus, a pulse is generated at intervals of exactly 20 μm. By counting these pulses, the scan motion reverses at the proper position. These encoder pulses are also used to command the A/D converters to sample the detector outputs. Since each pulse is generated at a precise position of the mirrors, data from successive scans can be coadded for greater reliability and noise reduction. Actually data sampling must be at a higher rate than the basic encoder resolution so these pulses are accurately subdivided by a phase lock loop. In normal optical encoder applications of this type, the light sources and detectors for the encoder are located outside the dewar and optical fibers transmit the signals. Launch environment requires rugged caging and locking to prevent damage. The dihedrals are quite large (about 8 in. high) and heavy (about 1.5 lb each) and must withstand launch vibrations. Protection is provided by moving the platform beyond its normal stroke and by locking into a pair of cones and sockets. A latch motor rotates a roller shaft deflecting a leaf spring which forces the cones into the sockets. As further protection, each flex pivot is fitted with a sleeve which limits deflection in the lateral direction.

REQUIREMENTS

The performance and operational requirements that the MTM was designed to are the following:

(1) Slow scan, 0.228 cm/sec
(2) Rapid scan, 0.342 cm/sec
(3) Flyback, $\geq$1.5 cm/sec
(4) Power dissipation, <5 mW
(5) Dynamic platform tilt (Table I)
(6) Operating temperature, 1.8 K (LHe)
(7) 26-g load vector design criteria
(8) Vibration test specifications (Table II)
(9) Jitter - 40 μsec
(10) Space constraints within FIRAS instrument
(11) Long scan platform travel, -0.4096 to 1.638 cm
(12) Short scan platform travel, -0.4096 to 0.102 cm

All optical and structural components, where possible, are constructed from 6061-T6 aluminum to prevent stresses and distortions upon cooldown to LHe temperatures.

SELECTION PROCESS

Prior to the selection of the flex pivot mechanism there was an evaluation period in which three basically different mechanisms were investigated. They consisted of a linear ball slide, flexural pivot-four-bar linkage, and a magnetic suspension platform.

The linear ball slide consisted of a platform riding on two parallel shafts through three linear ball bushings. Basically two configurations were built and tested. The first had stainless steel rods without lubrication and the second had aluminum shafts with a hard coat and teflon lubrication burnished onto the shafts. Although the power to drive the platform was low, the noise present on each linear sweep was unacceptable from an optical data analysis standpoint. The stainless steel version was tested first and had the highest noise levels. To try and reduce the noise, hard coated aluminum shafts with a Teflon burnished coating were substituted for the stainless shafts. The noise levels were reduced but were still unacceptable. Another potential problem with this mechanism was that it had to be kept exceptionally clean since contamination on the shafts or bearings would greatly increase power and noise values.

The magnetically suspended interferometer platform (Fig. 11) was designed, built, and tested. Magnetic suspension provides a very smooth, frictionless mounting which can be quite stiff with no restoring force in the direction of motion. Each of three bearing assemblies (Fig. 12) is a square unit with a central hole for the moving shaft. A permanent magnet in each corner sets up flux paths as shown. The flux in opposite air gaps can be differentially changed by winding coils on pole pieces. Depending on current direction total flux at the top gap is increased, while flux in the bottom gap is decreased. The result is a net upward force on the shaft. Coils are also provided on the horizontal poles so that force can be applied in either direction. Two of the magnetic bearings are in line, supporting a single long shaft. These bearings are controlled both vertically and horizontally. The third bearing supports a shorter shaft and is controlled only in the vertical direction.

Although testing of the unit showed good performance, it was not selected for the MTM because the flex pivot design was simpler and would meet the requirements.

The flex pivot mechanism was originally designed as a four bar linkage utilizing six flex pivots (Fig. 1). This mechanism was tested and found to have very smooth operation with extremely low power dissipation (Fig. 2). Because of the excellent operational characteristics and simplicity of design this mechanism was chosen for the MTM. Several design changes were made during the development and testing of this mechanism; however, because of

space limitation only the final version utilizing eight flex pivots will be discussed in detail in this report.

MECHANICAL DESIGN

The "BASIC DESIGN" mechanism described in this report will be the eight flex pivot four bar linkage (Fig. 3). Briefly this MTM was changed from a six flex pivot design to an eight flex pivot design to increase the rigidity of the dihedral mirror platform support. The original version provided two flex pivots in the movable connecting link which supported the dihedral platform. When the MTM was inverted, as was necessary during certain tests, there was interference with the gratings due to excessive deflections.

This six pivot model was redesigned and reanalyzed utilizing our NASTRAN modeling and analysis program to the present "BASIC DESIGN" MTM, herein referred to as MTM.

The MTM consists of the following major components and subsystems:

(1) Flex pivots, links, and base
(2) Latch mechanism
(3) LVDT and LVT sensors
(4) Fiber optics and grating
(5) Spherical mirror reflector
(6) Linear motor

In Figures 4 and 5 each of the major components is identified. Each of the four links has the holes for the flex pivots line bored so as to provide a true coaxial centerline for the pivot axes, thus eliminating rotational stresses due to misalignment. In addition the center distance of each pivot on corresponding links is located to very close tolerances so as to provide true translational motion of the movable connecting link. This is the link on which the dihedral platform is mounted and as such any rotational motion would be detrimental to the optical performance. The flex pivots are captivated in the links by slotting the bored holes, and with the use of a machine bolt, the hole is clamped about the pivot diameter. This provides a uniform clamping action without distorting the flex pivot. At LHe temperature the $\Delta\ell/\ell$ of aluminum is 0.0043 and that of stainless steel is 0.003; therefore, as the system is cooled the clamping force on the pivot is increased. Tests were conducted to determine whether the clamping force was sufficient to prevent the pivots from moving during vibration or whether we had to consider the use of an adhesive. Measurements taken at LN_2 temperatures showed that the push out force was in excess of 2224 N (500 lb) which was above any loads that would be seen during environmental testing. Initially, the pivots were mounted directly in the links; however, because of problems arising out of testing (to be discussed later) close toleranced sleeves are bonded to the pivots which limit the radial excursion and therefore the flexure deflections to a safe level. Another modification that was made was in the material used to fabricate the flex pivots. The standard material is a 400 series stainless steel; however, at LHe temperatures the impact resistance is very low <2.7 N-m (2 ft-lb). To insure a better impact strength at

cryogenic temperatures, INCO 718 was selected for the flex pivots. It has an impact resistance of about 27 N-m (20 ft-lb).

Since this mechanism is essentially frictionless and swings freely, it was necessary to design a latch mechanism that would captivate all moving components during the launch environment and yet be readily uncaged once in orbit and data taking is to begin. In addition it must be positioned such that it will not interfere with the MTM operation when uncaged. As shown in Figure 6 the caging mechanism consists of a 15° stepper motor operating through a 24:1 gear ratio. The output shaft is attached to an arm connected to the shaft at 90° with two special order "V" shaped bearings attached (one on each end). When the motor is engaged, the output shaft rotates and the two bearings each engage a beryllium copper leaf spring (Fig. 4) compressing it approximately 0.051 cm (0.020 in.). This results in approximately 311 N (70 lb) of force which is reacted by the latch cones and sockets (Fig. 7). The surfaces of the cones and sockets are hard anodized to prevent wear debris from forming. In addition, the cone angles were selected such that a self-locking tendency would not be present. Internal to the socket housing, a small spring is incorporated which is designed to give about a 8.9 N (2 lb) unlocking force to the cones so that when the latch motor releases the 311 N (70 lb) holding force the cones are kicked out of the sockets to ensure release. It should be noted here that in order not to have the latch motor assembly interfering with the MTM motion during operation the latch position is slightly out of the MTM operating range. In order to bring the leaf springs close enough to the latch motor for latching purposes, the linear drive motor is used for positioning into the latch cones.

The gear reduction consists of a pinion machined onto the output shaft of the motor, meshing with the two-pass gear system. The large gears are aluminum with a hard anodized surface lubricated with a burnished MoS_2 coating. Located within the gear box are two miniature electromagnetic proximity sensors which indicate the latch and unlatch positions.

The motor detent torque of 0.0177 N-m (2.5 in.-oz) is sufficient to prevent the gear box output shaft from rotating during handling environmental testing. For redundancy purposes the motor is constructed with dual windings, any one of which will be able to operate the latch/unlatch sequence.

Because of problems that arose during the tests, which will be discussed later, a third point-constraint was added (Fig. 8). This constrained point prevents the MTM dihedral platform and connecting link from rotating excessively about an axis through the latch cone assemblies.

As part of an overall mechanical analysis of the MTM a NASTRAN model was constructed. It consists of 665 grid points, 449 CQUAD's, 256 CBARS, 6 HEXA, 4 PENTA, and 109 CTRIA elements. The NASTRAN model is shown in Figure 9, which also shows a comparison of NASTRAN modes with measured modes indicating good accuracy of the NASTRAN model.

ENVIRONMENTAL TESTING AND MODIFICATIONS

Thermally, the MTM must survive launch conditions at LHe temperatures, and once in orbit it must operate at this temperature. Although we were able to performance test the MTM at LHe temperatures, vibration testing could only be done at LN_2 temperatures due to the test dewars that were available. The sequence for vibration testing was to perform a room temperature vibration and if everything was successful then an LN_2 vibration would follow. The reason for two separate tests was that the room temperature test was out in the open allowing clear visual observation during tests, but the LN_2 tests had the MTM mounted inside a dewar where no visibility was possible.

Vibrational testing consisted of (1) a sine burst test at about 20 cps to simulate the steady-state component of the vibration and (2) a random test. These tests were performed separately and in each of three mutually perpendicular directions. The vibration test specification levels used are shown in Table II.

As mentioned previously, there were two major problems that developed during the vibration testing that necessitated significant redesign in the latch mechanism. Loads were developed during testing which caused a rocking motion in the dihedral platform resulting in pivoting motion about the latch cone axis. This placed excessive loads on the pivot flexures causing them to fail.

To reduce this motion a third point latch was developed (Fig. 8) which limited motion to ±0.0051 cm (±0.002 in.). This was arrived at by a compromise of how tight a clearance could be maintained without possible binding and the allowable stress buildup in the flexures at that excursion. The third point latch consists of a slot in the latch motor housing and a tang attached to the rear of the dihedral platform connecting link. The spacing is adjusted so that when the tang is moved into the slot during the latch mode there is a clearance gap on each side of the tang of 0.0051 cm (0.002 in.). This arrangement was retested and worked.

Later in our test program there was a condition in which the MTM was vibrated but because of a misadjustment in the relationship of the latch motor to latch spring, the cones were not seated properly in their respective sockets. This allowed excessive motion at the sockets even though the third point latch was engaged. In effect, the platform could rotate about the third point latch. This caused failure in several pivots. At this point it was decided that the pivots themselves should be protected from excessive loads in case of another overload condition. After an extensive investigation it was decided to enclose each pivot in a sleeve (Fig. 10) that would limit radial movement to an acceptable level. This level was selected at a maximum of 0.0076 cm (0.003 in.) after an analysis showed a stress level of 248 MPa (36 000 psi) was reached with 0.0076 cm (0.003 in.) deflection and that buckling occurred at about 303 MPa (44 000 psi).

Testing in a fixture showed that buckling occurred slightly above 0.0076 cm (0.003 in.) which probably put the stress close to 303 MPa.

The sleeves were designed to have tightly machined tolerances so as to minimize the sleeve to sleeve dimensional variations. Taking into account the tolerances on the pivots, sleeves, and the center shift at 4° (rotation of flex pivot in latch position) of each pivot, a maximum radial clearance of 0.008 cm (0.0032 in.) and a minimum radial clearance of 0.0011 cm (0.00045 in.) are possible. The upper pivot section is bonded to the sleeve. Each sleeve and corresponding pivot have recessed grooves machined into the mating surface to allow for epoxy retention. Subsequent room temperature vibration testing showed no failed pivots.

An LN_2 vibration test is planned in early 1986 to verify cold temperature survival.

ELECTRICAL DESIGN

Drive and Control of MTM

The MTM operates in a closed-loop velocity mode, in which a velocity sensor feeds into the servoamplifier (Fig. 13). If a constant dc level is applied to the input, the motor will drive at a constant velocity such that velocity sensor output just matches the input. It will continue to move at constant velocity until the input is reversed, after which it will move at constant velocity in the opposite direction until it is again reversed.

Length of stroke is controlled by an optical encoder having 50 lines/mm. The encoder also generates a single zero reference pulse (ZRP) which synchronizes the operation. When the ZRP occurs during forward motion, a converter is set to zero and scan operation begins. Motion continues until the converter reaches 1024 counts. Distance travelled is exactly 20.48 mm, since encoder pulse spacing is 20 μm. When this point is reached, the MTM reverses and flies back at about five times the forward scan velocity.

When ZRP occurs during flyback, a time delay is initiated, after which the direction switches to forward and the cycle repeats. The purpose of the time delay is to ensure that all transients are settled out and operation is smooth by the time ZRP is reached, at which point the next scan begins.

Figure 14 shows the four scan modes which can be selected: LONG FAST, LONG SLOW, SHORT SLOW, AND SHORT FAST. For short scans, forward motion reverses after 256 counts or 5.12 mm. For slow scans, reference voltage is exactly 2/3 the value of FAST scans.

An additional mode of operation is the POSITION mode, in which a position sensor (LVDT) feeds into the servoamplifier and is balanced out by a position-command voltage which can be sent by telemetry. Since this is sent as an 8-bit word, the MTM can be set to any of 256 discrete positions. It will stay in this position until a new value is sent or until operation is returned to the normal SCAN mode.

Drive Motor

The drive motor (Fig. 15) was designed for a stroke of about 30 mm (1.2 in.) and a diametral clearance of about 1.5 mm (0.060 in.). This large clearance provides for the arc movement of the arms and for dimensional changes due to temperature or imperfect alignment.

The moving part, attached to the MTM platform, is completely passive and consists of four powerful rare-earth magnets at each end, forming an annular air gap, north inward at one end, north outward at the other end. A coil at each end cuts these magnetic lines, generating a push-pull force which is essentially linear over its range of travel. The coils are attached to the base, so the lead wires do not flex.

Initial motor design used niobium titanium wire, which becomes superconducting below about 9.5 K. The MTM was tested and operated at 4.5° with a motor of this type. However, some anomalies were noted: an apparent increase in spring constant and a large hysteresis effect. Because of these poorly understood factors, it was decided to redesign the motor, using normal copper wire, if power dissipation could be made low enough.

Since copper has finite resistance it was important to reduce the required current as much as possible by maximizing motor force constant. Redesign included the following:

(1) Samarium cobalt magnets were replaced with neodymium-iron, a newly developed material having about 50 percent higher gauss-oersted product.

(2) The flux return path was at or near saturation. Cross sectional area was increased about 50 percent.

(3) Overall diameter was increased to allow for 30 percent more turns.

Each coil of the final motor design is wound with 2600 turns of number 38 copper wire. With two coils in series (normal coils) there is a total resistance of about 830 ohms at room temperature, decreasing to about 10 ohms at LHe temperature. Redundant coils have the same number of turns, but resistance is 10 to 15 percent higher. The force constant is about 2.6 kg/amp (5.7 lb/amp) and the back EMF is about 27 mV/mm/sec. These same figures apply to either normal or redundant coils.

Optical Encoder

The optical encoder consisting of a scale and a reticle is shown in Figure 17. The scale is mounted on the moving platform and the reticle is attached to the base. Optical fibers are positioned directly below the encoder parts. Those below the scale feed light in from external light sources. A spherical mirror is mounted so that its radius of curvature is in the plane of the gratings. This mirror images the scale pattern onto the reticle, and the fibers below the reticle pick up the fringe pulses and carry them out to external detectors. For reliability, two complete sets of

optics and electronics are provided, only one of which is used at a time. Both F and Z are normal components, F_2 and Z_2 are redundant.

Both scale and reticle are spring loaded against two edges and the backside since differential expansion between the glass and aluminum due to temperature cycling would result in a position shift.

In conventional encoders, scale and reticle face each other with a small space between. Light passes through the grating patterns and fringe modulation is sensed by a detector. However, spacing between scale and reticle has a large effect on signal output, as shown in Figure 16(a). If nominal spacing is 0.005 in., scale movement of even 0.001 in. can double or halve the peak-to-peak signal. A further disadvantage is that such close spacing between precision glass surfaces is hazardous, particularly in ground handling and testing. Figure 16(b) shows the encoder arrangement used in the MTM. The reticle is separated from the scale and has its pattern in the same plane as that of the scale. Light passes through the scale to a spherical mirror which images the scale pattern back onto the reticle.

The spherical mirror used in the MTM is ground to 1/4 wavelength accuracy and is made of aluminum, as is the tower supporting it. Thus, as distance between mirror and scale (4-in. focal length) contracts due to the cold temperature, the radius of curvature contracts in proportion so that the pattern remains in focus.

Optical Connectors

Three types of connectors are used:

(1) A hermetic feedthrough connector which penetrates the dewar wall

(2) A blind-mating connector to permit installation and removal of the cryo-optical assembly

(3) A connector to permit removal of the MTM from the cryo-optical assembly (see Fig. 17)

Figure 18 shows the hermetic feedthrough connector. A vacuum-tight seal is accomplished by a Koval disc into which glass inserts are fused and then ground and polished to form clear windows. Ground and polished fibers are inserted from each side and butted against the glass windows. Attenuation is about 5 dB/pass through the connector.

The blind-mate connector is a butt joint connector in which one-half is mounted in a floating arrangement and guided by tapered pins into alignment with the other half. Attenuation is about 3 dB/pass.

The MTM optical connector permits separation of the MTM from the interferometer and COA assembly. Alignment pins insure accurate butt connection of fibers. Attenuation is about 3 dB/pass.

Optical Fibers

The optical fibers selected for this application are large diameter plastic fibers (DuPont Crofon, 1 mm diam). By using such large diameter fibers, the problems in designing and using connectors are greatly eased. These fibers have a high attenuation (about 0.5 to 0.6 dB/ft). However, they are minimally affected by bending, cryogenic temperature, or radiation.

For evaluation of bending and temperature effect, fibers were wrapped around mandrels of successively smaller radius and exposed to cryogenic temperature. The same fiber was used for all the tests, and temperatures were applied by plunging the fiber directly into the cryogen. After wrapping the fiber around each mandrel, it was dipped directly into liquid nitrogen and allowed to stabilize. Attenuation was read, after which it was immersed directly into liquid helium and read again. After warm up to room temperature, it was wrapped around the next smaller mandrel. Figure 19 shows the results. The fibers showed no sign of cracking or crazing.

Radiation received by the fibers during a year in orbit will amount to about 4000 rads. In testing, the fiber was subjected to a total of 80 000 rads with very little adverse effect.

Optical Preamp Box

Light sources and detectors are housed in the optical preamp box which is located near the dewar and connected to it by optical fibers. The preamp box contains a total of four LED's and four detectors, plus circuitry to control LED current and to amplify the detector signals. Half of these components are for the normal system and half are for the backup redundant system.

The LED's are high-power gallium arsenide diodes which are constructed with a lens. Rated output is 30 mW at 200 mA, although it was decided to limit current to 100 mA for further reliability. The wavelength is 940 nm. Another lens concentrates the output further and an optical fiber is positioned to couple into it as much light as possible. A photo diode monitors a portion of the LED output and feeds into an automatic control circuit to maintain constant output.

Velocity Sensor (LVT)

The velocity sensor consists of a pair of coils with a permanent magnet core, which generates a voltage when the core is moved axially. Output is proportional to velocity and is essentially linear over its range of travel. To get optimum linearity, core magnets are measured and selected for best uniformity of magnetic field. For reliability, two sets of windings are provided. Sensitivity is about 6 mV/mm/sec for either winding.

Position Sensor (LVDT)

A conventional type linear variable differential transformer is used to measure position. Excitation is about 3.6 kHz and output is converted to dc by a demodulator and op amp. Linearity is about 0.5 percent over its range of 1 in. Redundant windings are provided.

Electronics

Almost all circuitry utilize CMOS devices for two reasons: (1) power requirements are very low, and (2) radiation resistance is adequately high.

TABLE I. - DYNAMIC PLATFORM TILT

AXIS	P.D.(CM)	ALLOWABLE ROTATION (ARC-SEC)	P.T. (CM)	P.T. (IN)
Y	±.2 ± 1 −1 to 5	± 8 ± 20 ± 204	±.058 ±.289 −.289 to 1.45	±.023 ±.114 −.114 to .571
X	±.2 ± 1 −1 to 5	± 16 ± 40 ± 408	±.058 ±.289 −.289 to 1.45	±.023 ±.114 −.114 to .571
Z	NOT SPECIFIED			

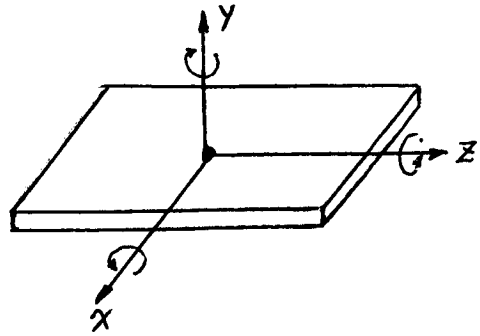

PLATFORM TRAVEL

TABLE II. - VIBRATION TEST LEVELS

	X	Y	Z
RANDOM (GRMS)	6.75	3.8	3.3
SINE BURST (G's)	10.0	10.0	10.0

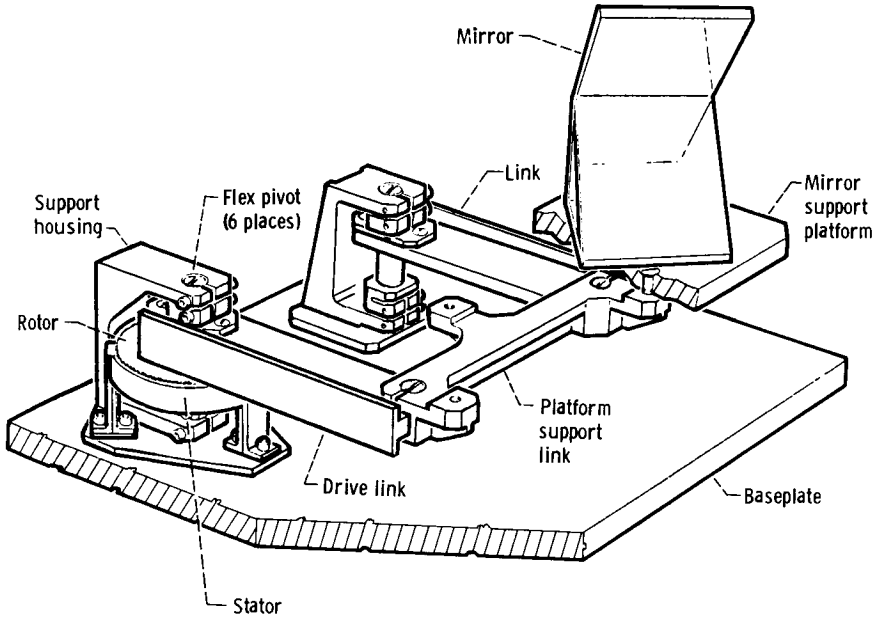

Figure 1. - Original MTM design.

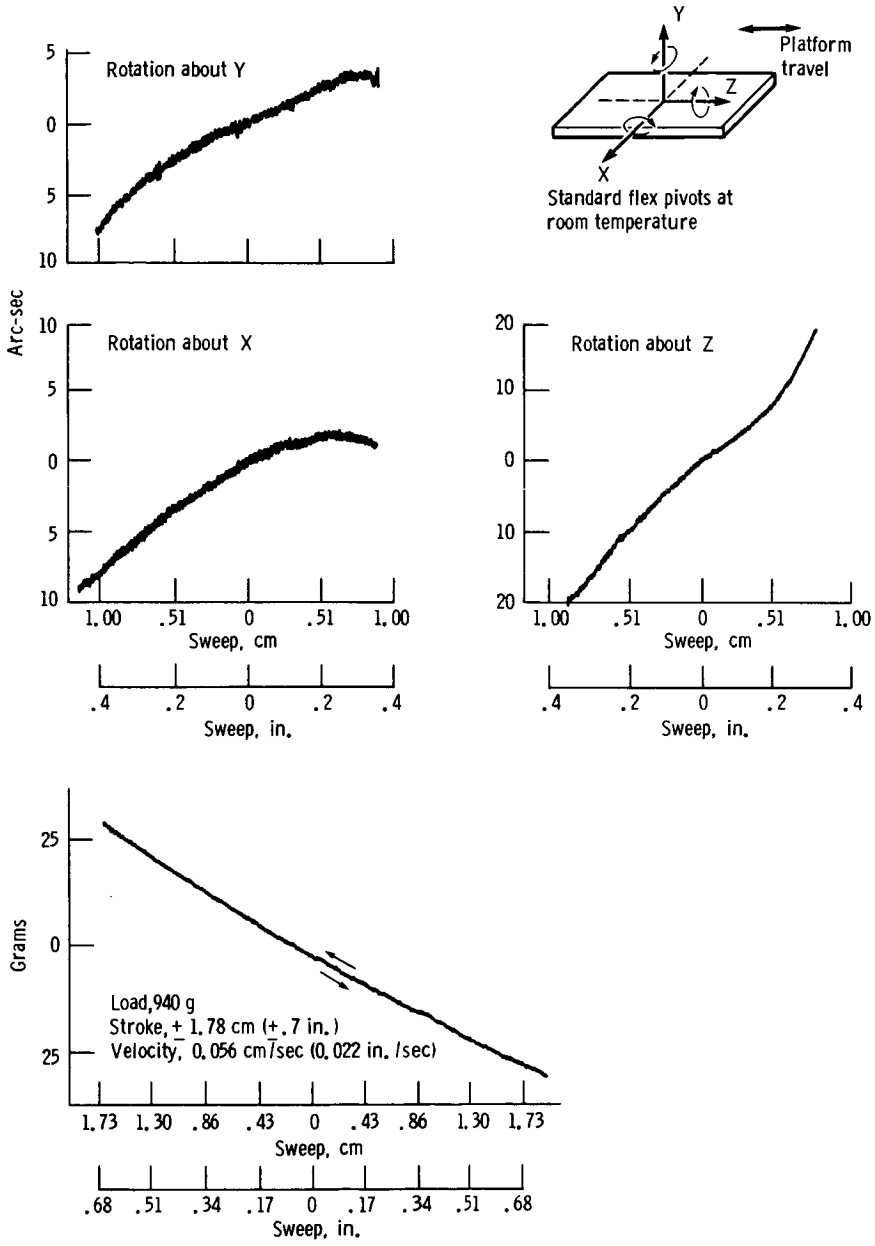

Figure 2. - Flex pivot mechanism operational characteristics.

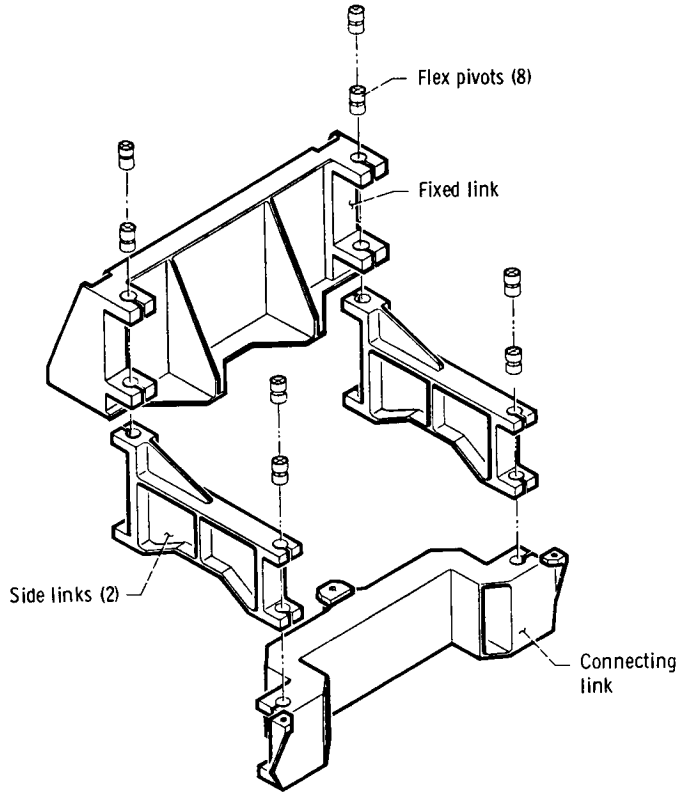

Figure 3. - MTM exploded view.

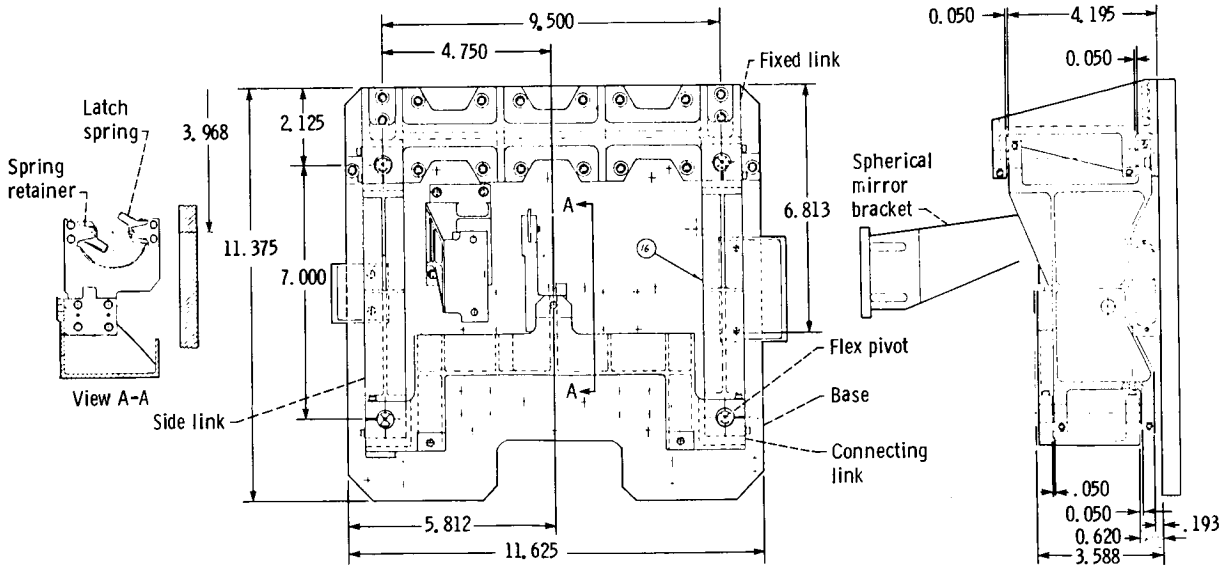

Figure 4. - MTM chassis assembly.

Table A

Position	Gap
At ZPD	.032 min
At STOW	.017
At EDT +	.002

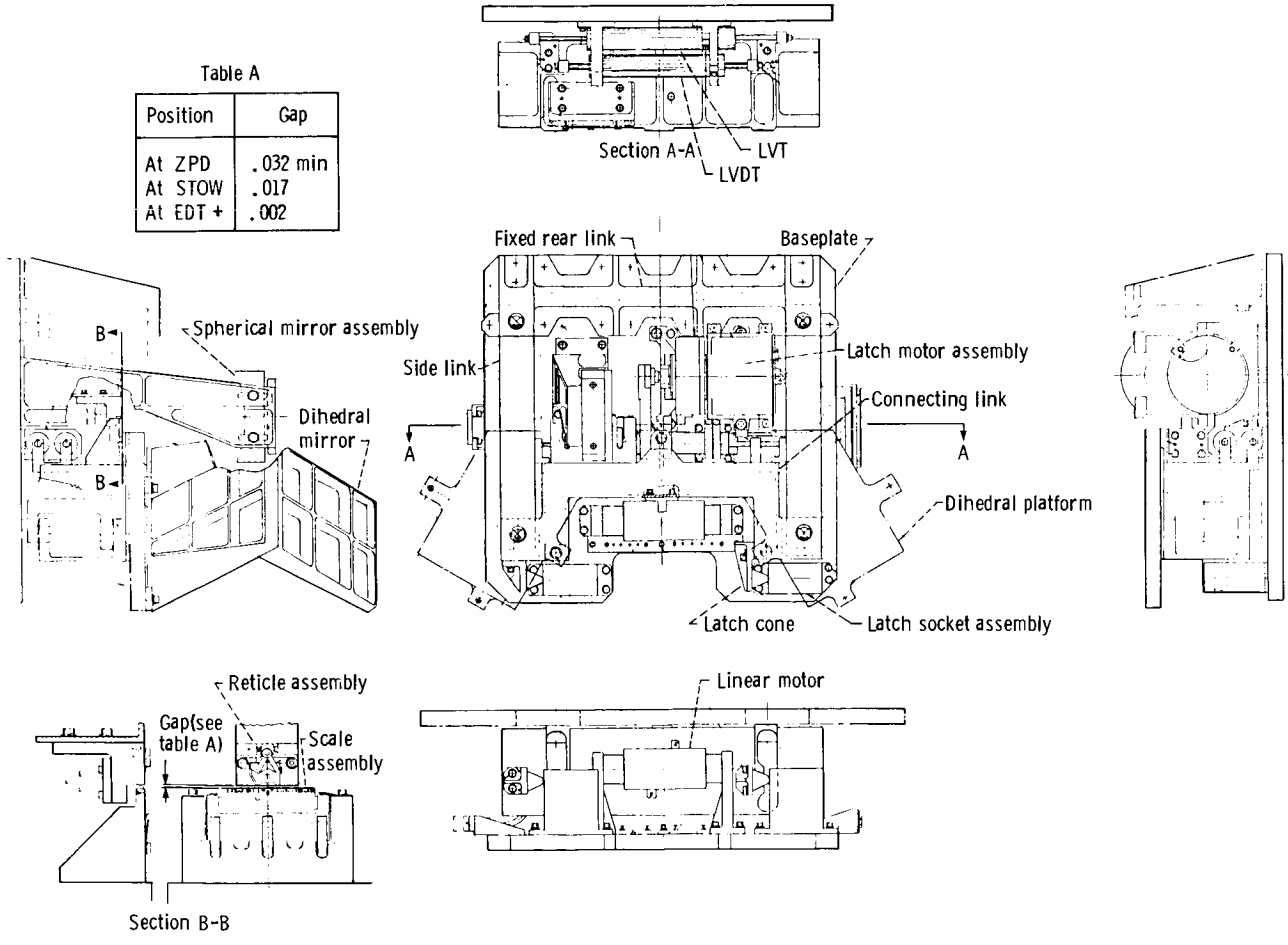

Figure 5. - Mirror transport mechanism assembly.

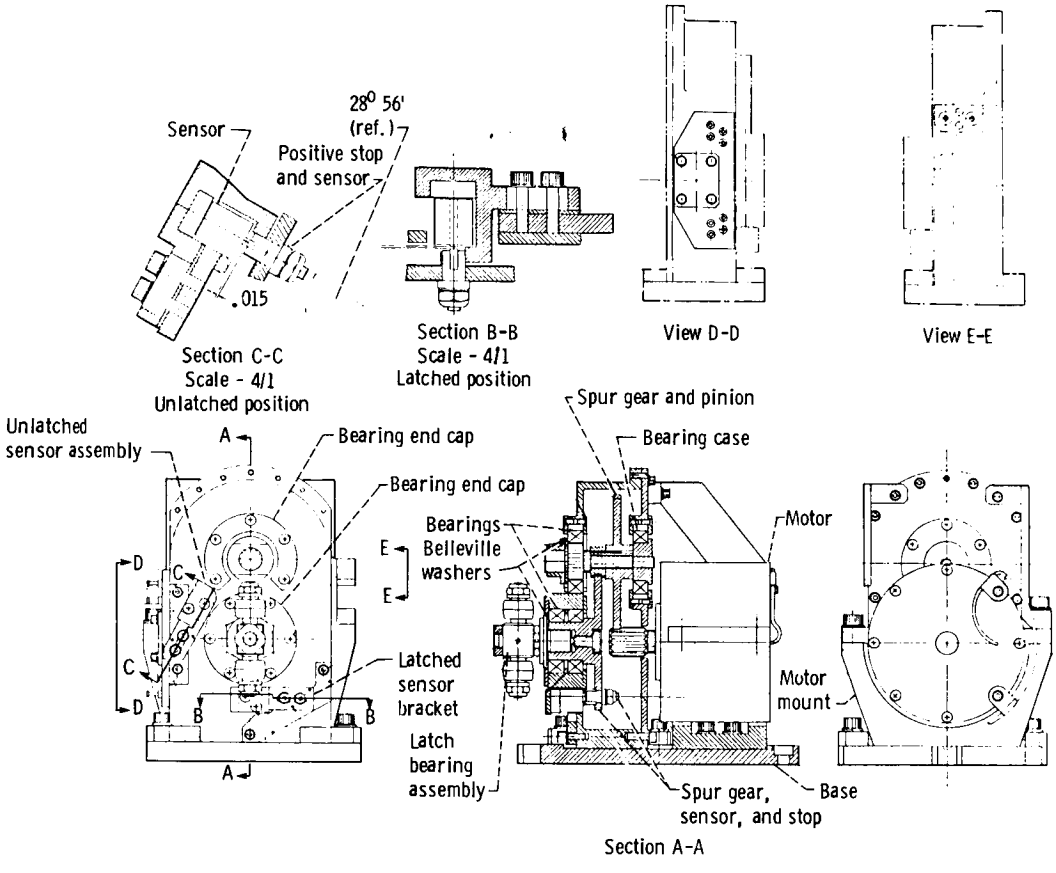

Figure 6. - MTM latch mechanism assembly.

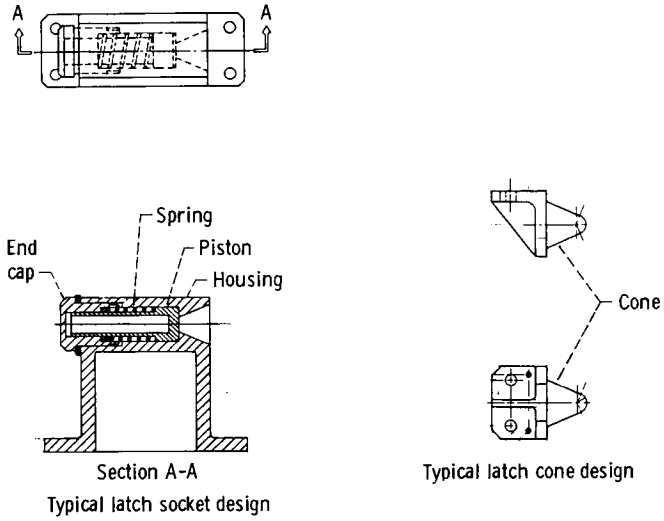

Figure 7. - Passive latch assembly.

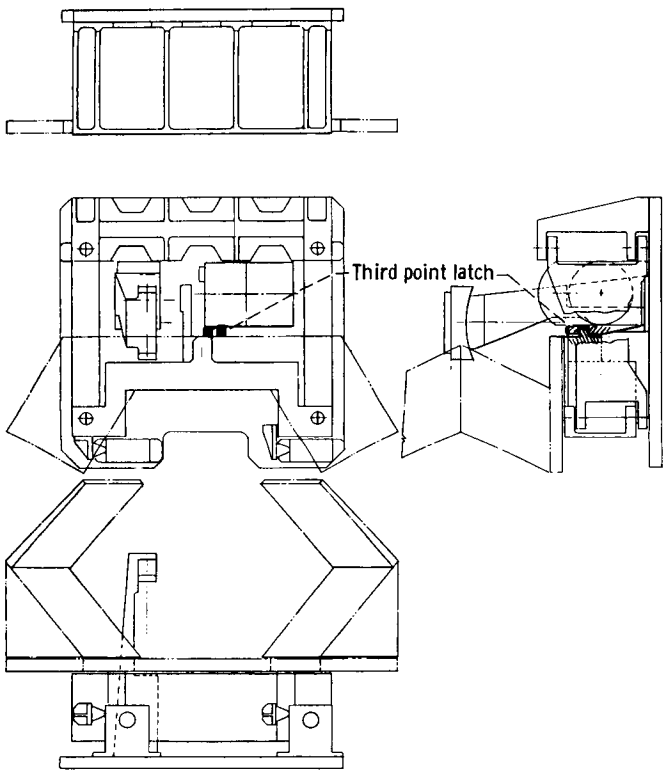

Figure 8. - Third point latch location.

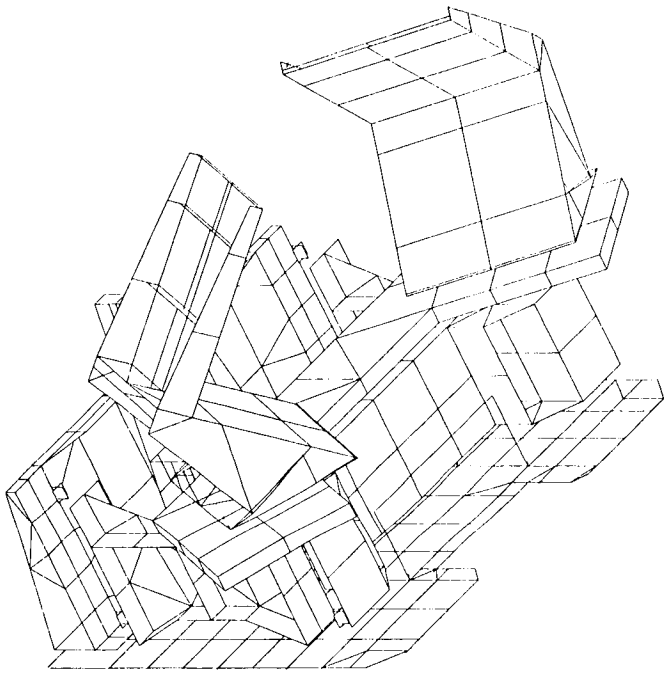

MTM Resonant frequencies

(Baseplate constrained by edges)

	Modes, Hz	1	2	3	4
Dihedral mirrors	Experimental	.581.63	46/49	---	---
	Nastran	.477	48.1	55.5	67.2

Figure 9. - Nastran model of MTM and correlation with test results.

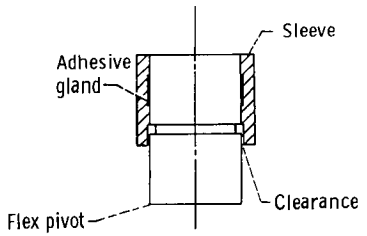

Figure 10. - Flex pivot sleeve assembly.

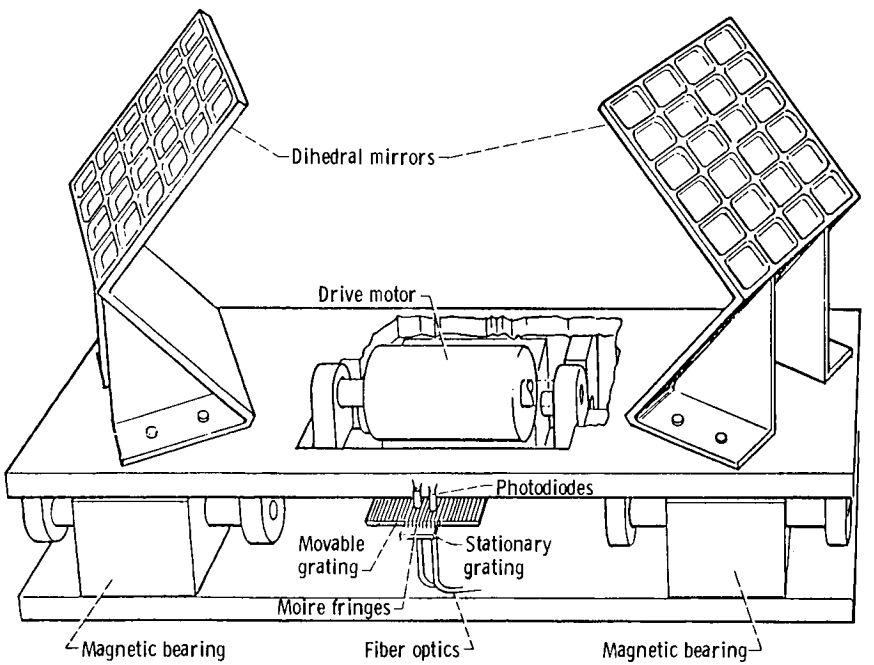

Figure 11. - FIRAS interferometer (magnetic suspension).

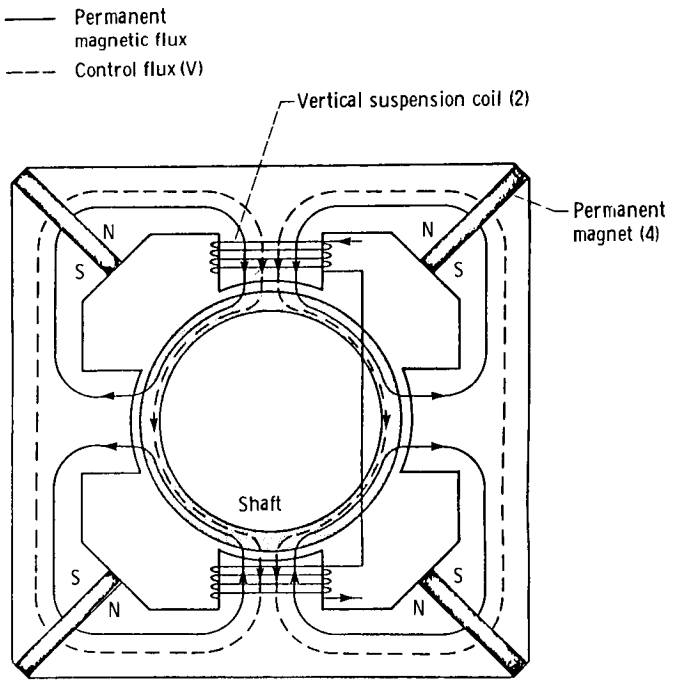

Figure 12. - Magnetic bearing. Current shown drives shaft up.

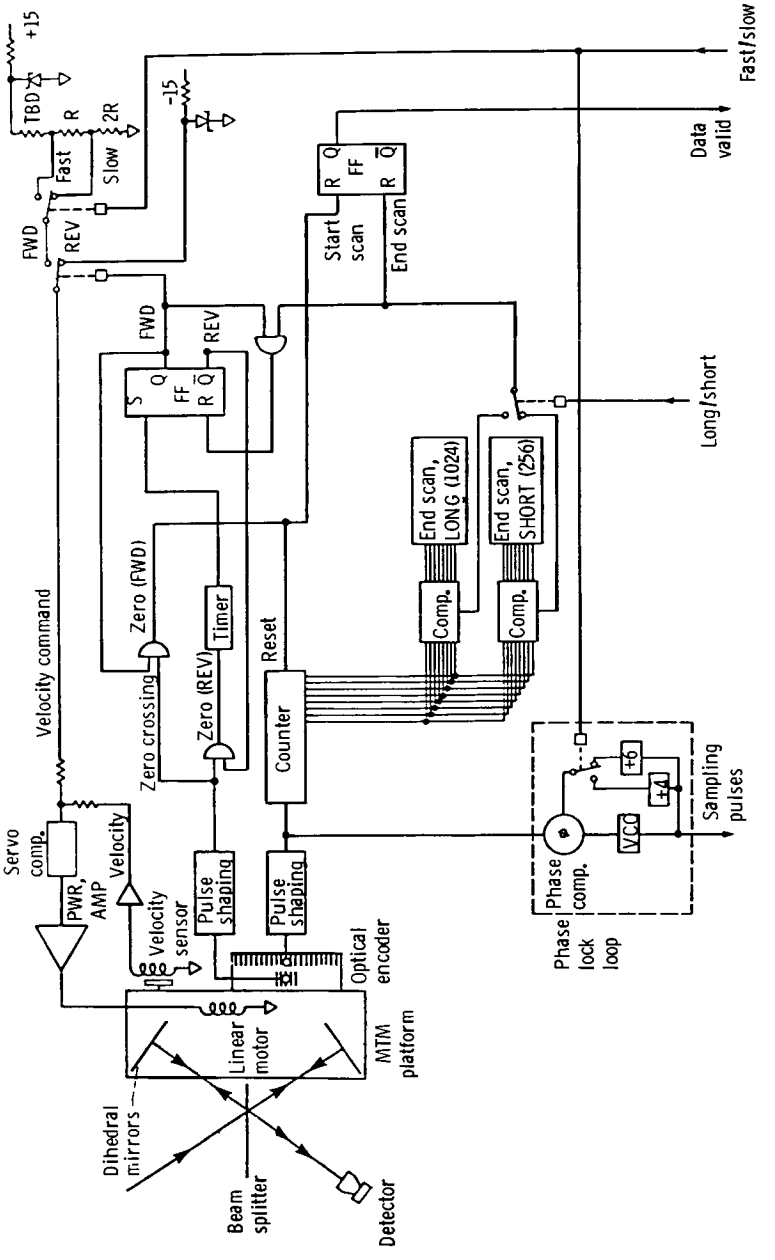

Figure 13. - FIRAS - MTM schematic.

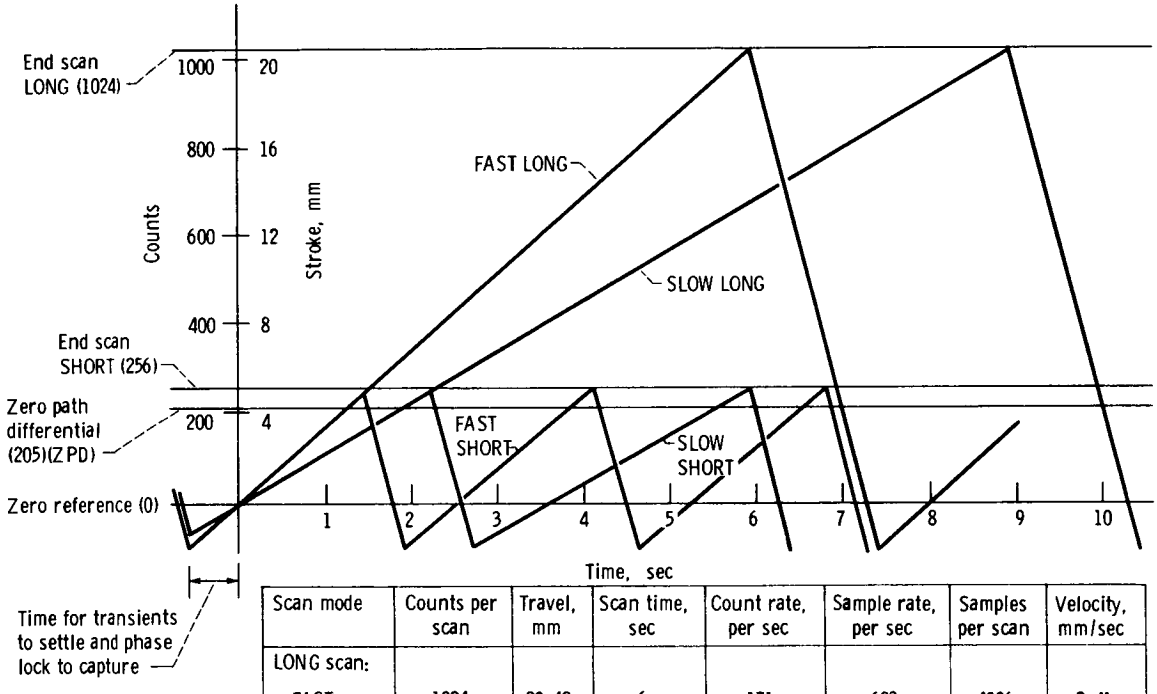

Scan mode	Counts per scan	Travel, mm	Scan time, sec	Count rate, per sec	Sample rate, per sec	Samples per scan	Velocity, mm/sec
LONG scan:							
FAST	1024	20.48	6	171	683	4096	3.41
SLOW	1024	20.48	9	114	683	6144	2.28
SHORT scan:							
FAST	256	5.12	1.5	171	683	1024	3.41
SLOW	256	5.12	2.25	114	683	1536	2.28

Figure 14. - FIRAS scan modes.

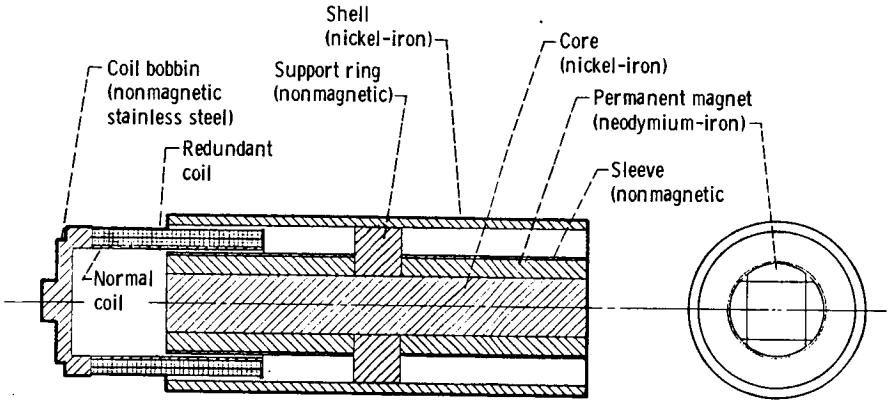

Figure 15. - Linear motor.

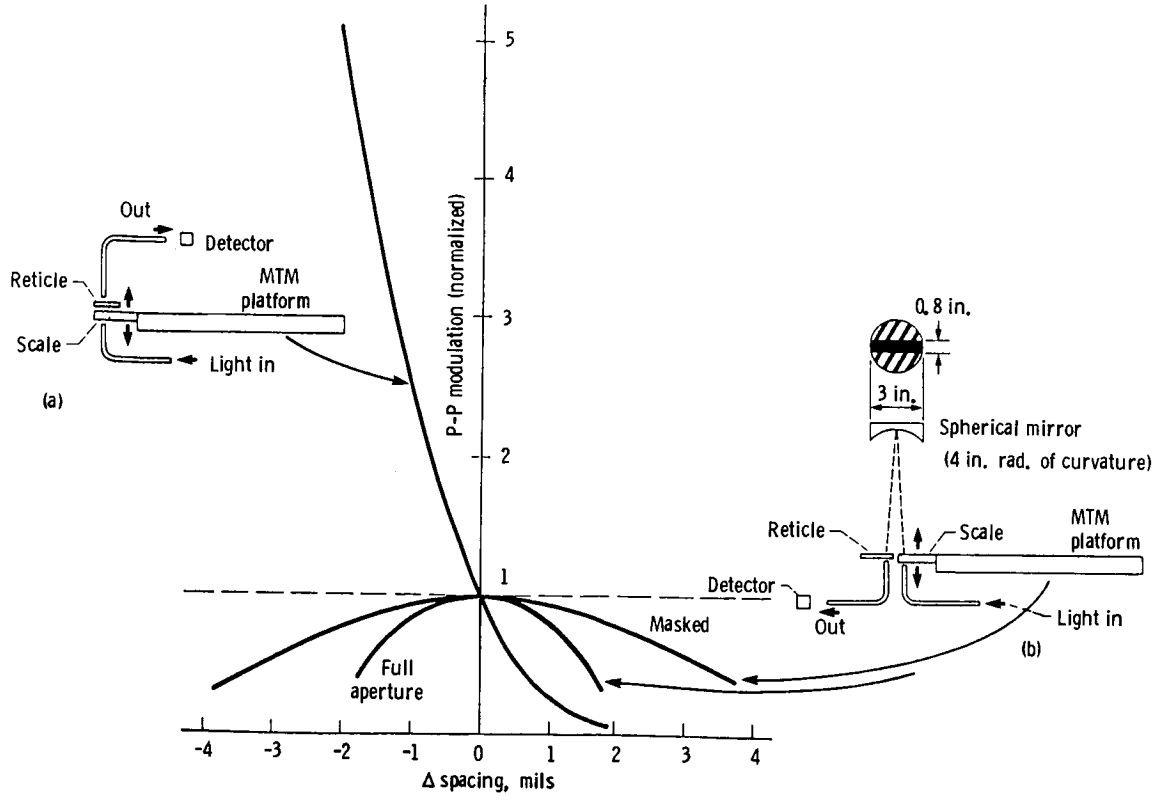

Figure 16. - Effect of grating spacing.

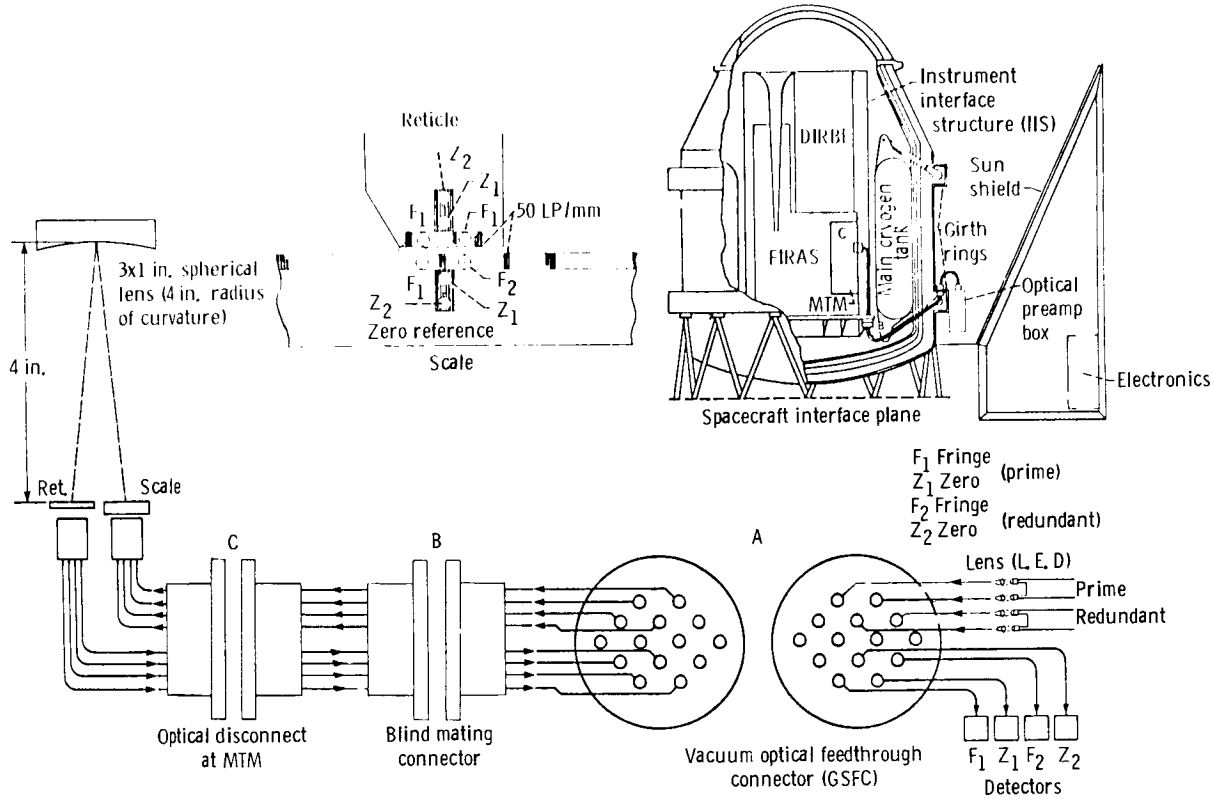

Figure 17. - Optical connectors and fiber optic routing.

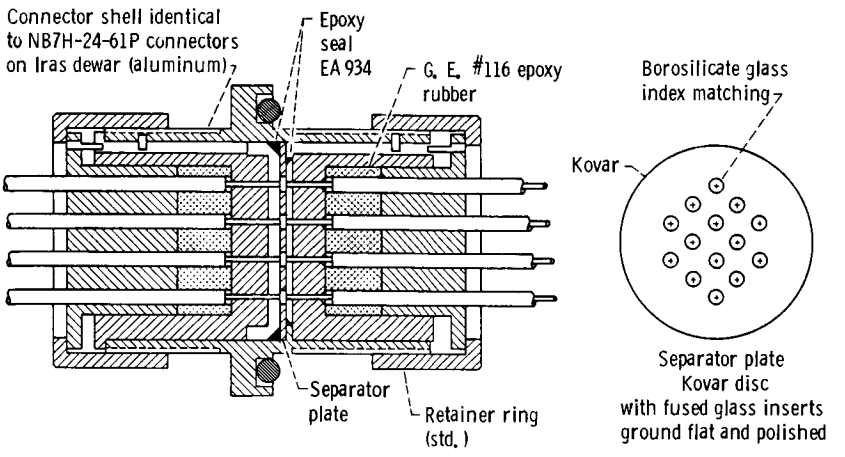

Figure 18. - Vacuum optical feedthrough connector.

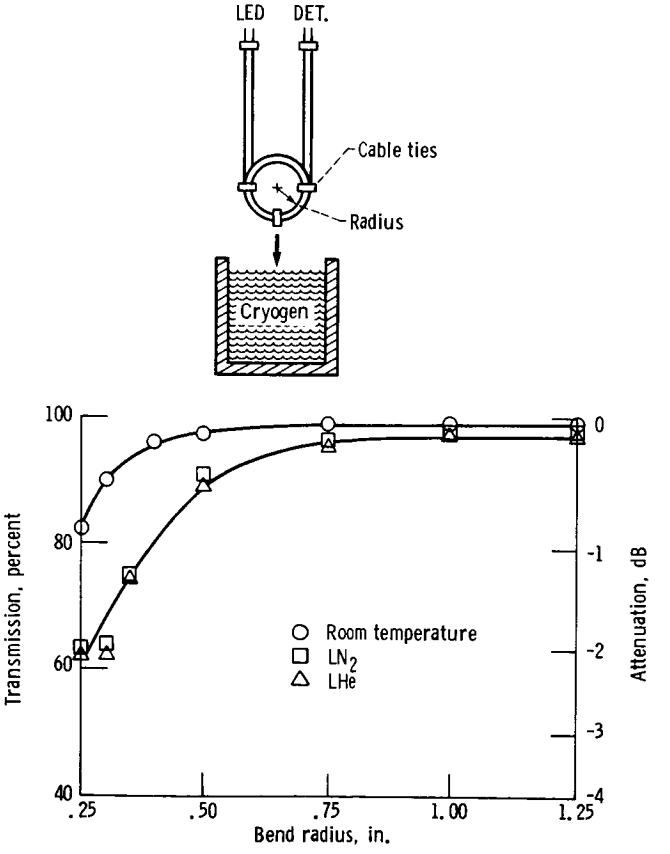

Figure 19. - Optical fiber performance. Fiber, DuPont Crofon OE-1040, 1-mm diameter.